

Mass spectrum of the butadiynyl radical (C_4H ; $X^2\Sigma^+$)

Xibin Gu, Ying Guo, Ralf I. Kaiser*

Department of Chemistry, University of Hawai'i at Manoa, 2545 McCarthy Mall, Honolulu, HI 96822, USA

Received 29 June 2005; received in revised form 28 July 2005; accepted 29 July 2005

Available online 6 September 2005

Abstract

We utilized the crossed molecular beams method to synthesize the butadiynyl radical, $C_4H(X^2\Sigma^+)$, via the reaction of dicarbon molecules with acetylene, under single collision conditions. Time-of-flight spectra of the radical were recorded at the center-of-mass angle (31°) of the parent ion ($m/z=49$; C_4H^+) and of the fragments at $m/z=48$ (C_4^+), $m/z=37$ (C_3H^+), and $m/z=36$ (C_3^+). This yields relative intensity ratios of $I(m/z=49):I(m/z=48):I(m/z=37):I(m/z=36):I(m/z=25):I(m/z=24)=1.0:0.67\pm 0.07:0.47\pm 0.06:0.2\pm 0.02:0.08\pm 0.02:0.04\pm 0.02$ at 70 eV electron impact energy. Signal at $m/z=13$ (CH^+) and 12 (C^+) contribute less than 0.04 relative to the parent peak; the intensity of the ^{13}C isotopic peak of the butadiynyl radical at $m/z=50$ ($^{13}C^{12}C_3H^+$) depicts an intensity of 0.04 ± 0.01 relative to $m/z=49$. Employing linear scaling methods, the absolute ionization cross section of the butadiynyl radical was computed to be $8.8\pm 1.8\times 10^{-16}$ cm². These data can be employed in future space missions to detect the butadiynyl radical in oxygen-poor combustion flames and in the atmospheres of planets (Jupiter, Saturn, Uranus, Neptune and Pluto) and their moons (Titan, Triton and Oberon) in situ via matrix interval arithmetic assisted mass spectrometry.

© 2005 Elsevier B.V. All rights reserved.

Keywords: Electron impact ionization; Fragmentation pattern; Mass spectrum; Free radical

1. Introduction

Free hydrocarbon radicals are important intermediates in combustion flames [1–3], astrochemistry [4], and planetary atmospheres [5,6]. Among the hydrogen-deficient radicals, the butadiynyl molecule, $C_4H(X^2\Sigma^+)$, has received particular attention. Detected in 1978 in the circumstellar envelope of the dying carbon star IRC+10216 [7] and subsequently in the taurus molecular cloud [8] (TMC-1) and photon-dominated regions [9], the butadiynyl radical was observed to be more abundant than many common molecules such as cyclopropenylidene ($c-C_3H_2$) and diacetylene ($HCC-CCH$) [10–12]. Both in the terrestrial settings like combustion flames [13] and extraterrestrial environments such as the interstellar medium [14] and planetary atmospheres [15–17], the butadiynyl radical has also been suggested as a precursor to complex polycyclic aromatic hydrocarbons (PAHs) and possibly fullerenes like C_{60} [18].

Despite the importance of the butadiynyl radical in combustion processes and in the chemical evolution of hydrocarbon rich planetary atmospheres, the mass spectrum of this molecule is still elusive [19]. However, a detailed knowledge of the fragmentation pattern will help to monitor combustion flames in real time and to determine absolute radical concentrations not only via spectroscopic techniques (Fourier transform microwave spectroscopy [20]; laser induced fluorescence [21]) and trapping techniques in cryogenic matrices [22], but also via mass spectrometry coupled to an electron impact ionizer. In terrestrial based laboratories, gas chromatography–mass spectrometry (GC–MS) serves as a powerful tool for off-line analyzes of complex gas mixtures [3]. Adapting GC–MS efficiently to planetary missions, however, suffers from a fundamental limitation. This ex situ technique excludes identification of thermally labile molecules, e.g., cyclobutadiene, C_4H_4 , or reactive radicals such as butadiynyl, which decompose in the GC capillary or react with the coating material. Therefore, these radicals cannot be sampled via GC–MS techniques. Reactive intermediates, however, play an important role in photochemistry of

* Corresponding author. Tel.: +1 808 9565730; fax: +1 808 9565908.
E-mail address: kaiser@gold.chem.hawaii.edu (R.I. Kaiser).

outer planets of our solar system [23]. Therefore, an alternative detection scheme of these important intermediates in the atmospheres of planets and their moons is clearly desired. Recently, a combination of quadrupole mass spectrometry (QMS) with matrix interval arithmetic (MIA) has been shown to extract the chemical composition of complex gas mixtures on line and in situ even in the presence of thermally labile molecules [24]. To extend this approach to the detection of radicals, the fragmentation patterns of these molecules such as of the butadiynyl radical are critical. For instance, signal at $m/z = 49$ from C_4H^+ – the parent ion of the butadiynyl radical – can be contaminated from the fragmentation of more complex hydrocarbons such as diacetylene (C_4H_2) and benzene (C_6H_6), which are very common in planetary atmospheres [23]. Therefore, the ion current recorded at, for instance, $m/z = 49$ (I_{49}), presents actually the sum of the ion currents of j molecule contributing to this mass-to-charge ratio each of them holding a partial pressure of p_j (Eq. (1)) (the j f_{49j} values represent the proportionality constants)

$$I_{49} = \sum_j f_{49j} \times p_j \quad (1)$$

Therefore, if the fragmentation patterns and the ionization cross section of the butadiynyl radical are known, the proportionality constants can be computed [24] and, hence, matrix interval arithmetic can be carried out to determine the concentrations of hydrocarbon radicals such as of the butadiynyl molecule in the atmospheres of planets and their moons. Note that in principle, selective photoionization utilizing a tunable ultraviolet photon source – a soft ionization technique which effectively eliminates the fragmentation of the radical cation to smaller fragments – coupled to a mass spectrometric device is feasible to reveal the time dependent concentrations of radicals in combustion flames [25]. However, since this technique requires a tunable vacuum ultraviolet light source – either a synchrotron or four wave mixing schemes – this method can hardly be utilized to identify the butadiynyl radical in the framework of an in situ exploration of hydrocarbon-rich atmospheres of planets and their moons via space crafts. Here, due to the size, weight, and power consumptions and potential misalignments of the optical elements of the laser system induced by the vibrations of the spacecraft during the launch, it would be a challenge to include a VUV laser system. Therefore, mass spectrometry coupled with matrix interval arithmetic presents a viable alternative in the in situ probing of planetary atmospheres.

In this paper, we obtain the mass spectrum of the butadiynyl radical which is synthesized in situ in a crossed molecular beams experiment. The crossed molecular beams technique represents the most versatile approach in the elucidation of the energetics and chemical dynamics of elementary reactions [26]. In contrast to bulk experiments, where reactants are mixed, the main advantage of a crossed beams approach is the capability to form the reactants in separate, supersonic beams. The reactants of each beam are made to

collide only with the molecules of the other beam, and the products formed fly undisturbed towards the detector. These features provide an unprecedented approach to observe the consequences of a single collision event and even to *synthesize* unstable radicals, preventing secondary collisions and wall effects.

2. Experimental setup

We generated the butadiynyl radical, $C_4H(X^2\Sigma^+)$, in a crossed molecular beams reaction of the dicarbon molecule, $C_2(X^1\Sigma_g^+/a^3\Pi_u)$, with acetylene, $C_2H_2(X^1\Sigma_g^+)$. Briefly, the main chamber of the crossed beams machine consists of a 2300 l, 304 stainless steel box and is evacuated by three 2000 l s^{-1} magnetically suspended turbo molecular pumps backed by a single scroll pump (10 l s^{-1}) to the low 10^{-8} Torr region. To reduce the background from straight-through molecules into the detector, the vessel is equipped with a cold shield located between the chopper wheel and the interaction region, downstream the skimmer. This oxygen free high conductivity (OFHC) copper shield is interfaced to the first stage (10 K) of a cold head and reduces the vacuum in the main chamber to 4×10^{-9} Torr. This arrangement keeps the pressure in the main chamber during an actual experiment to about 5×10^{-8} Torr. Two source chambers are located inside the main chamber; in its current geometry, both beams cross perpendicularly. Each source chamber is pumped by a 2000 and 430 l s^{-1} maglev pump to the medium 10^{-9} Torr region; operating pulsed sources increases the pressure to about 10^{-5} to 10^{-4} Torr. A dry roots pump (140 l s^{-1}) roughed by two oil-free EcoDry pumps (16 l s^{-1}) backs the turbo pumps of each source chamber.

A pulsed supersonic beam of dicarbon, $C_2(X^1\Sigma_g^+/a^3\Pi_u)$, was generated via laser ablation of graphite at 266 nm [27]. The 30 Hz, 20 mJ output of a Spectra Physics GCR-270-30 Nd:YAG laser is focused onto a rotating carbon rod. Ablated dicarbon molecules are seeded into helium carrier gas released by a Proch-Trickl pulsed valve operating at 60 Hz and $80\ \mu\text{s}$ pulses with 4 atm backing pressure. A four-slot chopper wheel located between the skimmer and the cold shield selects a segment of the seeded dicarbon carbon beam with a peak velocity of $1660 \pm 2\text{ ms}^{-1}$ and a speed ratio S of 5.5 ± 0.1 . The pulsed dicarbon and the pulsed acetylene beam (550 Torr backing pressure; $v_p = 902 \pm 2\text{ ms}^{-1}$; $S = 16.2 \pm 0.1$) pass through skimmers and cross at 90° in the interaction region of the scattering chamber.

The time-of-flight spectra of the fragmentation patterns of the butadiynyl radical were recorded in the plane of both beams using a rotatable quadrupole mass spectrometer with an electron-impact ionizer at the center-of-mass angle of the reaction of 31° . The Brink-type electron impact ionizer [28] is surrounded by a liquid nitrogen shield and is located in the third region of a triply differentially pumped ultra high vacuum chamber (10^{-11} Torr) (Fig. 1); the quadrupole mass filter and the Daly-type scintillation particle detector [29] are

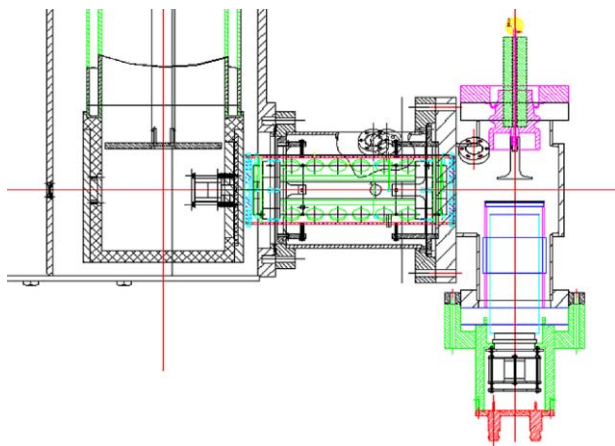


Fig. 1. Side view of detector system of the crossed beams machine utilized to determine the fragmentation patterns of the butadiynyl radical.

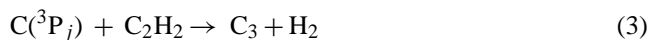
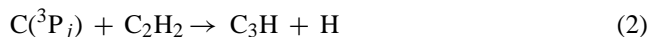
connected to the second region. Each region is pumped by a magnetically levitated turbo molecular pump (4301 s^{-1}); all three pumps are backed by a 4301 s^{-1} turbo molecular pump whose exhaust is connected to an oil free scroll pump (101 s^{-1}). This pumping scheme reaches down to the low 10^{-11} Torr in region three; lower pressures down to the high 10^{-13} Torr regime can be achieved by operating a cold head inside region three (4 K; 1.5 W). It is important to stress that the fragmentation patterns of a molecule strongly depend on the kinetic energy of the electron. Here, we recorded the fragmentation patterns at 70 eV electron energy, i.e., the *standardized* electron energy utilized to setup the NIST mass spectral database.

We also would like to address briefly the potentials of the ionizer. The actual ionizer consists of a thoriated iridium filament spot welded to a gold plated stainless steel cylindrical can, a meshed wire grid, and an extractor lens held at -150 V . The ion energy was held at $+36\text{ eV}$. Extracted ions are focused by an electric lens located after the extractor plate and pass the quadrupole mass filter and are accelerated towards a stainless steel target maintained at -25 kV . The ion hits the surface and initiates an electron cascade which is accelerated by the same potential until they reach an organic scintillator whose photon cascade is detected by a photomultiplier (PMT) mounted outside the UHV detector and held at -1350 V . Each PMT pulse passes a discriminator set at 1.5 mV to eliminate low-level noise and is then converted to a TTL signal. The latter is fed into a multichannel scaler (MCS) to record the time-of-flight spectra at distinct mass-to-charge ratios of the butadiynyl radical and its fragments.

3. Results

We would like to address now the experimental strategy to record the fragmentation patterns. In this context, it is important to note that the ablation beam does not contain only the desired dicarbon molecule, but also carbon atoms, $\text{C}({}^3\text{P}_j)$, and

tricarbon molecules, $\text{C}_3(\text{X}^1\Sigma_g^+)$ [27]. However, the tricarbon molecules do not interfere because their reaction with acetylene only takes place if the collision energy is larger than 86 kJ mol^{-1} [30]; in the present experiment, we selected a collision energy of 26.9 kJ mol^{-1} to eliminate any reactive scattering signal from the reaction of acetylene with tricarbon. On the other hand, the reaction of ground state carbon atoms with acetylene is very rapid within gas kinetics and proceeds via two exoergic and barrier-less pathways (2)–(3) [31]



Actually, there exist two C_3H isomers: the linear ($\text{D}_{\infty\text{h}}$) and the cyclic structure ($\text{C}_{2\text{v}}$). The formation of the cyclic isomer is exoergic by 8.6 kJ mol^{-1} , whereas the linear isomer is energetically less favorable by $6\text{--}7\text{ kJ mol}^{-1}$. The second channel to form tricarbon and molecular hydrogen holds an exoergicity of 160 kJ mol^{-1} . On the other hand, reactive encounters of dicarbon with acetylene have shown to open up only the butadiynyl plus atomic hydrogen channel (Eq. (4)) [32]



But how it is feasible to discriminate if the signal originates from the reaction of carbon atoms with acetylene or from dicarbon molecules colliding with acetylene? Signal at $m/z = 49$ (C_4H^+) and $m/z = 48$ (C_4^+) comes exclusively from the reaction of dicarbon with acetylene. However, ions at lower mass-to-charge ratios of, for instance, $m/z = 37$ (C_3H^+), could come from reaction (2) (reactive scattering signal) and (4) (fragmentation of the butadiynyl radical). To differentiate these pathways, it is useful to carry out a transformation of the coordinate system from the laboratory – in which the experiment is actually carried out – to the center-of-mass frame. The center-of-mass (CM) reference system is useful to gain information on the reaction dynamics. Here, the observer actually rests on the center-of-mass and observes (i) how the dicarbon collides with the acetylene molecule and (ii) in which direction the butadiynyl radical and the hydrogen atom departs. Fig. 2 summarizes the relationship between both coordinate systems.

In the experiment, a beam of the dicarbon with a lab velocity V_{C_2} crosses a beam of acetylene with a lab velocity $V_{\text{C}_2\text{H}_2}$ at 90° ; both velocities are represented as velocity vectors. The vector connecting the tips of the dicarbon and acetylene velocity vectors defines the relative velocity vector \mathbf{g}

$$\mathbf{g} = V_{\text{C}_2} - V_{\text{C}_2\text{H}_2} \quad (5)$$

In the laboratory system, the center-of-mass frame moves with the velocity V_{CM} calculated with the masses of the reactants m_{C_2} and $m_{\text{C}_2\text{H}_2}$ to Eq. (6). With respect to the dicarbon beam, this vector holds a fixed center-of-mass angle, θ_{CM} ,

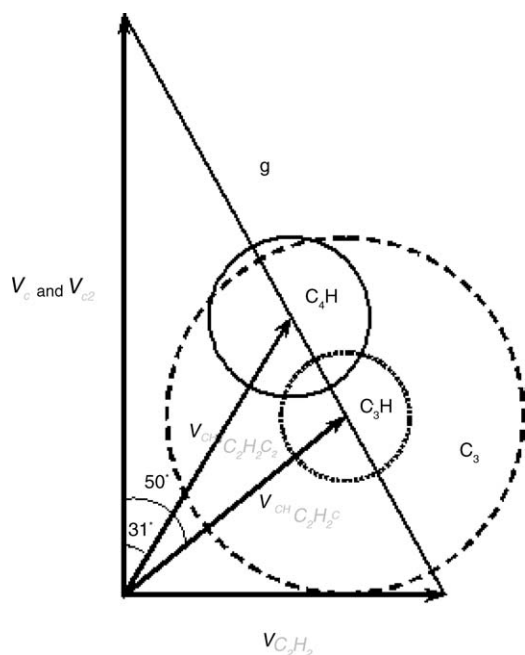


Fig. 2. Newton diagram of the reactions of carbon atoms and dicarbon molecules with acetylene via Eqs. (2)–(4). The maximum recoil velocities of the butadiynyl (C_4H), tricarbonhydride (C_3H), and tricarbon (C_3) are depicted as solid, dotted and dashed circles. See text for a detailed definition of the symbols.

(Eq. (7))

$$V_{CM} = \sqrt{\frac{(m_{C_2} V_{C_2H_2})^2 + (m_{C_2H_2} V_{C_2H_2})^2}{(m_{C_2} + m_{C_2H_2})^2}} \quad (6)$$

$$\Theta_{CM} = \arctan \left(\frac{m_{C_2H_2} V_{C_2H_2}}{m_{C_2} V_{C_2}} \right) \quad (7)$$

This gives the center-of-mass angles of 31° and 50° for the reactions of acetylene with dicarbon and atomic carbon, respectively. The center-of-mass velocity vector starts at the crossing point of the reactant beams and terminates at the center-of-mass of the system, which is actually located on the relative velocity vector g . Since we have two reactions – those of acetylene with dicarbon and atomic carbon – simultaneously, we also have to define two center-of-masses, $CM_{C_2H_2/C_2}$ and $CM_{C_2H_2/C}$, which are both located on the relative velocity vector g (Fig. 2). These center-of-masses play a central role to discriminate if the signal at lower mass-to-charge-ratios actually originates from reaction (2)–(4), alone or a combination of these channels. To distinguish between these possibilities, we must have a closer look at the energetics of each reaction. This is carried out here exemplarily for the reaction (2) assuming solely the cyclic C_3H isomer is formed. The total, maximum available energy, $E_{available}$, of the reaction, which can be released in translational energy of the reaction products, is simply the sum of the collision energy, E_c (Eq. (9)), plus the absolute of the exoergicity of

the reaction, $\Delta_R G^\circ$

$$E_{available} = E_c + |\Delta_R G^\circ| \quad (8)$$

$$E_c = \frac{1}{2} \left(\frac{m_{C_2H_2} \times m_C}{m_{C_2H_2} + m_C} \right) (V_{C_2H_2}^2 + V_C^2) \quad (9)$$

Energy and momentum conservation dictates how the available energy will be partitioned among the C_3H and H reaction products. Here, the maximum velocity of the heavy fragment in the center-of-mass reference frame, u_{C_3H} , can be calculated via the following equation:

$$u_{C_3H} = \left[\frac{2E_{available}(m_{C_3H} + m_H)}{m_{C_3H} \times m_H} \left(\frac{m_{C_3H}^2}{m_H^2} + 1 \right)^{-1} \right]^{1/2} \quad (10)$$

This presents the maximum recoil velocity a c - C_3H product can have in the center-of-mass system. Theoretically, the product molecules can scatter in a sphere, which is centered at the center-of-mass of the reaction; this sphere holds a radius of a velocity vector u_{C_3H} . Projecting the sphere into the two-dimensional velocity vector diagram (Fig. 2) around the center-of-mass of the reaction yields a circle with a radius of u_{C_3H} (dotted circle). A similar procedure can be carried out to calculate the maximum recoil velocities of the tricarbon product (Eq. (3); dashed circle) and of the butadiynyl radical (Eq. (4); solid circle). A detailed inspection of these recoil circles, the so called *Newton circles*, provides vital guidance for the experiment. Let us follow a line from the crossing point of the ablation and the acetylene beam along the center-of-mass of the velocity vector of the dicarbon plus acetylene reaction – placed 31° relative to the dicarbon vector – to the center-of-mass of the reaction. Here, we will see that this line passes first the Newton circle of the tricarbon reaction product (reaction (3)) and then the Newton circle of the butadiynyl radical (reaction (4)). Most importantly, this line does not cross the Newton circle of the C_3H reaction product. Therefore, the time-of-flight spectra of butadiynyl ($m/z=49$; C_4H^+) and its fragmentation patterns at $m/z=48$ (C_4^+), $m/z=37$ (C_3H^+), $m/z=36$ (C_3^+), $m/z=25$ (C_2H^+), $m/z=24$ (C_2^+), $m/z=13$ (CH^+) and $m/z=12$ (C^+) can show only interference from the tricarbon reaction product at mass-to-charge ratios of 36, 24, and 12. Hence, signal at $m/z=37$ comes predominantly – except an isotopic contribution of 3.3% from $^{13}C^{12}C_2^+$ – from fragmentation of the butadiynyl radical.

Selected the time-of-flight spectra recorded at the center-of-mass angle of 31° are shown in Fig. 3. Here, the time-of-flight spectra taken at $m/z=49$, 48, and 37 are – after scaling – super imposable. This underlines the conclusion drawn from Fig. 2 that ions at these masses come from the C_4H^+ parent and from the C_4^+ and C_3H^+ fragments. It is obvious to see that the time-of-flight spectrum at $m/z=36$ has two contributions: a faster part from tricarbon formed in reaction (3) and a slower part which has the same patterns as the signal recorded at $m/z=49$ (reaction (4)). Therefore, the latter presents the contribution of the fragmentation pattern of the butadiynyl radical to $m/z=36$. By integrating

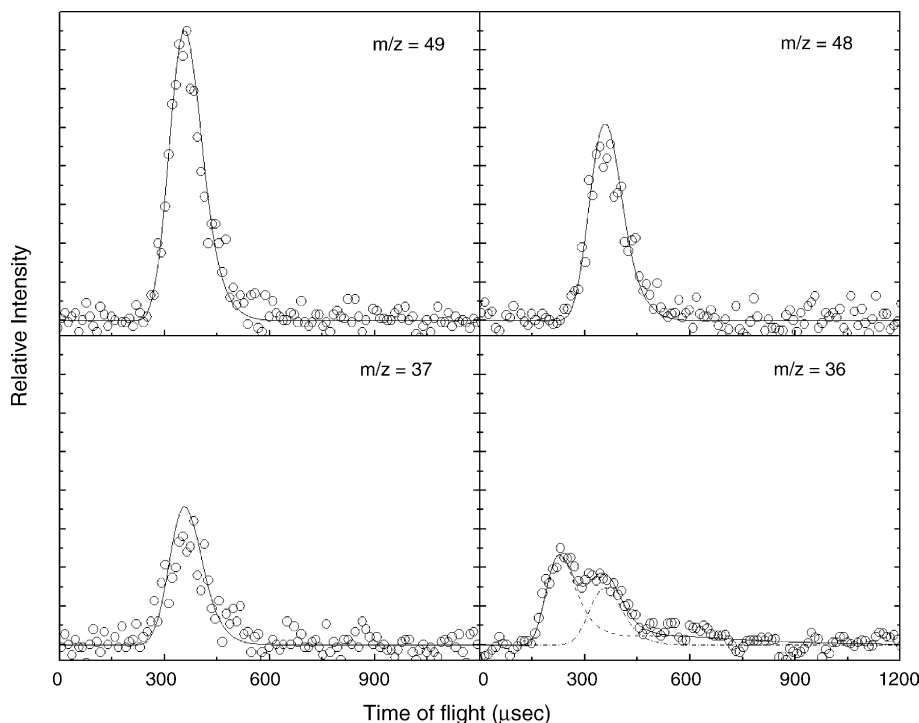


Fig. 3. Time-of-flight spectra of the butadiynyl radical at $m/z=49$ (upper left) and the most intense fragments at $m/z=48$ (upper right), 37 (lower left), and 36 (lower right). The circles represent the experimental data, the lines the fits derived from the dynamics of the carbon–acetylene (dashed line) [31] and dicarbon–acetylene (dash dot line) [32] systems. Data were taken with a mass resolution of 1 amu.

these time-of-flight spectra and normalizing them to the most intense peak, we yield the following intensity ratios of $I(m/z=49):I(m/z=48):I(m/z=37):I(m/z=36):I(m/z=25):I(m/z=24)=1.0:0.67 \pm 0.07:0.47 \pm 0.06:0.2 \pm 0.02:0.08 \pm 0.02:0.04 \pm 0.02$. We also recorded time-of-flight spectra at lower mass-to-charge ratios of 13 and 12. However, signal was less than 0.04 relative to the most intense parent peak of the butadiynyl radical at $m/z=49$. The synthesized mass spectrum of the butadiynyl radical is shown in Fig. 4.

Finally, we would like to present an approximation of the absolute, total ionization cross section of the butadiynyl radi-

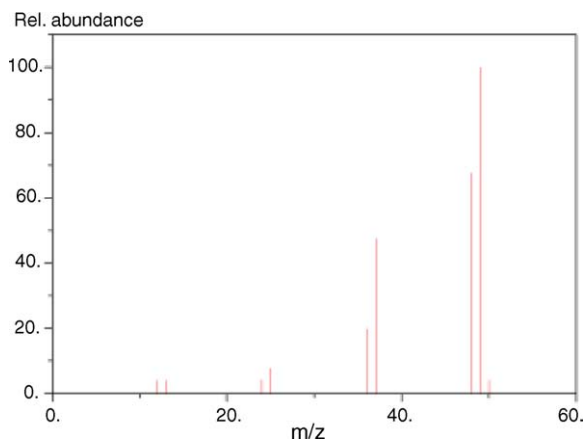


Fig. 4. Mass spectrum of the butadiynyl radical synthesized from the recorded parent peak and fragmentation pattern; the spectrum is presented in a NIST standardized format.

cal at 70 eV electron energy of. Here, in the range of 70–80 eV, the total electron impact ionization cross section, σ_{ion} , is – within $\pm 20\%$ – proportional to the averaged molecular polarizability, α [33]; the molecular polarizability is approximated as the sum of the atomic polarizabilities. Taking the atomic polarizabilities of carbon and hydrogen as $1.76 \times 10^{-24} \text{ cm}^3$ and $0.6668 \times 10^{-24} \text{ cm}^3$ [34], we can calculate the ratio of the cross section of acetylene to the butadiynyl radical to 0.63 ± 0.12 . Acetylene has been used as a reference because the structure of the acetylene molecule (carbon–carbon triple bond) and the butadiynyl radical are similar; further, the absolute ionization cross section of the acetylene molecule is known to be $5.5 \times 10^{-16} \text{ cm}^2$ at 70 eV [35]. This enables us to estimate the total, absolute ionization cross section of the butadiynyl radical to be $8.8 \pm 1.8 \times 10^{-16} \text{ cm}^2$.

4. Conclusions

The crossed molecular beams method was utilized to synthesize the butadiynyl radical, $\text{C}_4\text{H}(\text{X}^2\Sigma^+)$, via the reaction of dicarbon molecules with acetylene. Time-of-flight spectra of the radical were recorded at the center-of-mass angle of 31° at mass-to-charge ratios of $m/z=49$ (C_4H^+ ; parent ion) and the C_4^+ , C_3H^+ , and C_3^+ fragments at $m/z=48$, 37 and 36. Integrating these time-of-flight spectra and normalizing them to the most intense peak, intensity ratios of $I(m/z=49):I(m/z=48):I(m/z=37):I(m/z=36):I(m/z=25):I(m/z=24)=1.0:0.67 \pm 0.07:0.47 \pm 0.06:0.2 \pm 0.02:0.08 \pm$

0.02:0.04 ± 0.02 were obtained at 70 eV electron impact energy. Signal at $m/z = 13$ (CH^+), and 12 (C^+) contribute less than 0.04 relative to the parent peak. Also, the absolute ionization cross section of the butadiynyl radical has been determined to be $8.8 \pm 1.8 \times 10^{-16} \text{ cm}^2$. These data can be employed now in future space missions to detect the butadiynyl radical in the atmospheres of hydrocarbon rich planets (Jupiter, Saturn, Uranus, Neptune and Pluto) and their moons (Titan) and also in combustion flames via mass spectrometry coupled with matrix interval arithmetic. We would like to note that the actual fragmentation patterns also depend on the internal energy of the neutral molecule to be ionized. An investigation of the ratio of the fragmentation pattern of, for instance, $m/z = 49$ and 48 shows a very mild fluctuation of less than 5% over a collision energy range of 10–50 kJ mol^{-1} . This error could be included into the matrix interval arithmetic. Our approach presents a versatile strategy to synthesize free radicals under single collision conditions and to synthesize their mass spectra via their fragmentation pattern.

Acknowledgements

This work was supported by the US Department of Energy-Basic Energy Sciences (DE-FG02-03ER15411; XG, RIK) and by the National Science Foundation (CHE-0234461; YG, RIK).

References

- [1] J.H. Kiefer, S.S. Sidhu, R.D. Kern, K. Xie, H. Chen, L.B. Harding, *Combust. Sci. Technol.* 82 (1992) 101.
- [2] M. Hausmann, K.H. Homann, Proceedings of the 22nd International Annual Conference of ICT (1991) on Combustion Reaction Kinetics, 1991, p. 1.
- [3] H.Y. Zhang, J.T. McKinnon, *Combust. Sci. Technol.* 107 (1995) 261.
- [4] Y.C. Minh, E.F. van Dishoeck, *Astrochemistry: From Molecular Clouds to Planetary Systems*, Astronomical Society of the Pacific, San Francisco, 2000.
- [5] M.V. Sykes, *The Future of Solar System Exploration*, Astronomical Society of the Pacific, San Francisco, 2002.
- [6] M.E. Summers, D.F. Strobel, *ApJ* 346 (1989) 495.
- [7] M. Guelin, S. Green, P. Thaddeus, *ApJ Lett.* 224 (1978) 27.
- [8] P. Friberg, A. Hjalmarsen, W.M. Irvine, *ApJ Lett.* 241 (1980) 99.
- [9] O. Morata, E. Herbst, Some Time-dependent Results for PDR Chemistry, Special Publication SP-577, European Space Agency, 2005, p. 393.
- [10] T.J. Millar, P.R.A. Farquhar, K. Willacy, *Astron. Astrophys. Suppl. Series* 121 (1997) 139.
- [11] K. Hoshina, H. Kohguchi, Y. Ohsima, Y. Endo, *J. Chem. Phys.* 108 (1998) 3465.
- [12] S.D. Doty, C.M. Leung, *ApJ* 502 (1998) 898.
- [13] M. Hausmann, P. Hebgen, K.H. Homann, Proceedings of the 24th Symposium (International) on Combustion, 1992, p. 793.
- [14] D. Teyssier, D. Fosse, M. Gerin, P. Maryvonne, A. Abergel, E. Habart, Proceedings of the Conference, Waterloo, Ont., Canada, 21–23 August, 2002, 2003, p. 422.
- [15] F. Stahl, P.V.R.F. Schleyer, H.F. Schaefer, R.I. Kaiser, *Planet. Space Sci.* 50 (2002) 685.
- [16] L.M. Lara, R.R. Rodrigo, A. Coustenis, J.J. Lopez-Moreno, E. Chas-sefiere, European Space Agency, Special Publication SP-338, 1991, p. 137.
- [17] G. Gladstone, M. Allen, Y.L. Yung, *Icarus* 119 (1996) 1.
- [18] G.S. Hammond, V.J. Kuck, *Fullerenes*, American Chemical Society, Washington, DC, 1992.
- [19] <http://webbook.nist.gov/chemistry/>.
- [20] M. Nakajima, Y. Sumiyoshi, Y. Endo, *Rev. Sci. Instrum.* 73 (2002) 165.
- [21] K. Hoshina, K. Kenosuke, Y. Ohshima, Y. Endo, *J. Chem. Phys.* 108 (1998) 108.
- [22] C. Kubitzka, M. Schottler, K.H. Homann, *Berichte der Bunsen-Gesellschaft* 91 (1987) 695.
- [23] Y.L. Yung, W.B. DeMoore, *Photochemistry of the Planetary Atmospheres*, Oxford University Press, Oxford, 1999.
- [24] R.I. Kaiser, P. Jansen, K. Petersen, K. Roessler, *Rev. Sci. Instrum.* 66 (1995) 5226.
- [25] C.Y. Ng, *Vacuum Ultraviolet Photoionization and Photodissociation of Molecules and Clusters*, World Scientific, Singapore, 1991.
- [26] R.I. Kaiser, *Chem. Rev.* 102 (2002) 1309; A.F. Furlan, G.E. Hall, *J. Chem. Phys.* 109 (1998) 10390; A. Furlan, *J. Phys. Chem. B* 103 (1999) 1550; X. Yang, K. Liu, *Modern Trends in Chemical Dynamics*, World Scientific, Singapore, 2003; R.A. Dressler, *Chemical Dynamics in Extreme Environments*, World Scientific, Singapore, 2001.
- [27] R.I. Kaiser, A.G. Suits, *Rev. Sci. Instrum.* 66 (1995) 5405.
- [28] G.O. Brink, *Rev. Sci. Instrum.* 37 (1966) 857.
- [29] N.R. Daly, *Rev. Sci. Instrum.* 31 (1960) 264.
- [30] R.I. Kaiser, et al., *Faraday Discuss.* 119 (2001) 51.
- [31] R.I. Kaiser, C. Ochsenfeld, M. Head-Gordon, Y.T. Lee, A.G. Suits, *Science* 274 (1996) 1508.
- [32] R.I. Kaiser, N. Balucani, D.O. Charkin, A.M. Mebel, *Chem. Phys. Lett.* 382 (2003) 122.
- [33] R.L. Summers, Empirical observations of the sensitivity of hot cathode ionization type vacuum gauges, NASA Technical Note TN D-5285, 1969; R. Holanda, Sensitivity of hot cathode ionization vacuum gauges in several gases, NASA Technical Note TN D-6815, 1972.
- [34] *CRC Handbook of Chemistry and Physics*, National Institute of Standards, Boca Raton, 2004.
- [35] C. Tian, C.R. Vidal, *J. Phys. B* 31 (1998) 895.